

# *Investigation of electric field effect of bubble defects in XLPE high voltage cables*

Lingxin Zeng<sup>1</sup>, Shaoting Yuan<sup>2</sup>

<sup>1</sup>*School of Electronic, Electrical Engineering and Physics, Fujian University of Technology, Fuzhou, 350108, China*

<sup>2</sup>*School of Automation and Electrical Engineering, Lanzhou Jiaotong University, Lanzhou, 730070, China*

**Keywords:** XLPE Cable, Air Bubble Defect, Finite Element Software, Electric Field Strength

**Abstract:** High-voltage cross-linked polyethylene (XLPE) cables play a pivotal role in power systems owing to their unique advantages. Nonetheless, during cable operation, small bubble defects can arise from manufacturing imperfections or operational issues. Over time, these defects can distort the electric field within the cable, potentially leading to local breakdowns. To investigate the impact of bubble defects on the electric field distribution within XLPE cables, this study employs the COMSOL finite element software to construct a simulation model. Through this model, we simulate the electric field strength inside the cables and analyze its distribution characteristics. Additionally, we explore the effects of varying bubble sizes and positions on field strength distortion. Our findings reveal that a bubble diameter of 0.5mm in the XLPE cable results in electric field strength aberration. Furthermore, as the bubble size increases, the aberration in electric field strength becomes more pronounced. Similarly, as the bubble moves closer to the core end, the deviation in electric field strength intensifies, leading to a greater impact. The insights from this study offer valuable guidance for the operation and maintenance of actual cables.

## **1. Introduction**

With the development of modern electric power system, cross-linked polyethylene, abbreviated as XLPE. They are more and more widely used, due to its irreplaceable advantages, it has gradually replaced the overhead transmission lines. XLPE material has excellent insulation properties, long service life, and very good electrical and mechanical properties.<sup>[1]</sup> However, XLPE cables have many advantages, it is difficult to avoid bubble defects in the manufacturing, installation and operation process for some reasons, and eventually the failure of the cable.<sup>[2]</sup>

The existence of air bubble defects can result in localised field concentration. Over an extended period, this concentration can deteriorate the insulation properties of the XLPE material, ultimately leading to cable failure. In recent years, numerous scientists have undertaken comprehensive research on the electric field strength distribution in XLPE cables. Their investigations have particularly emphasized the impact of minor defects in cable joints and air gap imperfections on the electric field distribution.

Du Hao and colleagues explored the partial discharge traits of air gap imperfections in 10kV cross-linked polyethylene cables subjected to DC voltage. Their findings revealed a close correlation between the initiation voltage of partial discharge in air gaps and both the frequency and volume of discharges with the applied voltage. Gang Liu and Zhijuan Chen utilized electric field simulation software to examine the electric field distribution in the main insulation of a 10kV cross-linked polyethylene cable terminal containing air gap defects. Their results indicated an inverse relationship between the width of cable defects and the degree of E-field distortion, with the maximum E-field strength surpassing the standard specified value. Meanwhile, Cen Xu provided a concise analysis of the root causes of common failures in 10kV cross-linked polyethylene cables and suggested targeted preventive measures. Xu underscored the significance of cable failures in maintaining power system stability and stressed the need for proactive maintenance to ensure cable operation safety.

Although existing studies have provided a certain understanding of the electric field strength distribution characteristics within XLPE cables, they still lack systematic simulation analyses, especially the study of the differences in the effects of different positions and sizes of air bubbles on the electric field strength is still insufficient. Therefore, the purpose of this paper is to use COMSOL finite element software to establish the simulation model of XLPE cable, to study the electric field strength distribution characteristics inside the cable, and to focus on the differences between different bubble sizes and different bubble positions on the field strength distortion. Through the research in this paper, it is expected to provide a more comprehensive and in-depth reference basis for the operation and maintenance of actual cables.

In this paper, a realistic model of the XLPE cable is constructed within COMSOL to delve deeply into the distribution patterns of electric field strength within the cable. Through a systematic simulation analysis, a detailed comparison is drawn between the differential impacts of bubbles of varying sizes and positions on the distortion of electric field strength. The simulation outcomes unequivocally reveal that the existence of bubbles within the XLPE cable causes substantial distortion of the electric field strength. Furthermore, there is a direct correlation between bubble diameter and the rate of electric field strength distortion: larger bubbles result in more pronounced distortion effects on the electric field strength. Additionally, the bubble's location within the cable plays a pivotal role in electric field distortion. As the bubble approaches the core end, the distortion of electric field strength intensifies, potentially causing more severe damage. The findings from this study not only enrich the theoretical framework surrounding electric field distribution in cables but also offer a valuable theoretical foundation and reference for the operational maintenance of actual cables. This, in turn, aids in enhancing the safety and stability of cable operations.

The main innovations of this paper are as follows:

(1) Multi-dimensional analysis of bubble defects: In the simulation of bubble defects, the paper not only analyses the size of bubbles, but also explores the effect of bubbles at different locations on the electric field strength, and this multi-dimensional analysis provides a more comprehensive guide for practical applications.

(2) Refined simulation of electric field distribution: The electric field distribution inside the XLPE cable is refined using COMSOL finite element software, which can accurately reflect the influence of different bubble sizes and positions on the electric field strength, providing an important reference for subsequent manufacturing and maintenance of the actual cable.

(3) Comparative analysis of different bubble sizes and positions: Through the comparative analysis of electric field distortion of bubbles of different sizes and positions, the influence of bubble size and position on electric field distortion is found, which provides a theoretical basis for improving the safety and reliability of the cable.

## 2. The simulation model

### 2.1 Construction of a two-dimensional model of an XLPE cable

Single-core cross-linked polyethylene DC cables are usually made of a five-layer structure of copper conductor core, conductor shield, XLPE insulation, insulation shield and outer sheath, which are precisely extruded and moulded. To investigate the electric field intensity distribution in the steady state in an electrostatic field, we constructed a two-dimensional coaxial structure simulation model of the cross-linked polyethylene cable in COMSOL software. The structure of this two-dimensional model is clearly shown in Figure 1, while the properties of each material layer and its relative dielectric constant are listed in detail in Table 1. The finite element method (FEM) is a numerical computational method for solving the approximate solution of the partial differential equation boundary problem. Domestic power cables operate in a 50 Hz industrial AC environment where the electric field changes slowly with time and can be treated as an electrically quasi-static field.<sup>[3]</sup> We have used the following system of equations (1), (2) and (3) for the exact analysis.

$$\nabla \cdot D = \rho v \quad (1)$$

$$E = -\nabla V \quad (2)$$

$$J = \sigma E + j\omega D + J_e \quad (3)$$

Where:  $D$  is the conductor potential shift;  $\rho$  is the charge density;  $E$  is the electric field strength;  $V$  is the applied potential;  $J$  is the conducting current density;  $\sigma$  is the conductor conductivity (S/m); and  $J_e$  is the exogenous current density (A/m<sup>2</sup>).

Based on the relative permittivity of the insulating material with respect to free space, the intrinsic relationship between the electric field  $E$  and the potential shift  $D$  of the insulating material is:

$$D = \varepsilon_0 \varepsilon_r E \quad (4)$$

Where:  $\varepsilon_0$  is the dielectric constant of free space,  $\varepsilon_r$  is the relative dielectric constant of the insulating material.

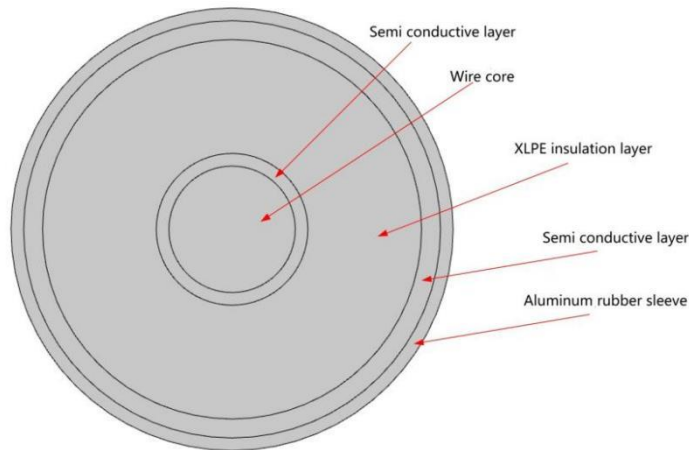


Figure 1: XLPE cable layout diagram

Model settings: the radius of the core is 5mm, the radius of the circle of its inner semiconducting layer is 5.7mm, the radius of the circle of the XLPE insulation layer is 10mm, the radius of the circle of the outer semiconducting layer is 11mm, and the radius of the circle of the aluminium rubber sleeve

is 12mm.

## 2.2 Simulation Parameters

Table 1: Materials and parameters of each layer

| Composition           | Material   | Relative Permittivity |
|-----------------------|--|-----------------------|
| Copper core           | copper   | 0.0001                |
| Semi conductive layer | silicone rubber                                      | 12                    |
| XLPE insulation       | Ultra-smooth semiconductor cross-linked polyethylene | 2.3                   |
| Insulating shield     | silicone rubber                                      | 12                    |
| Waterstop             | polyacrylate   | 3.5                   |
| Air gap               | air  | 1                     |
| Outer jacket          | aluminum   | 0.0001                |

## 2.3 Modelling of cable air gap defects

During the cable extrusion process, imperfections in the manufacturing process often result in air gap defects. These gaps can contain air, moisture, and other contaminants that can significantly impact breakdown strength. XLPE, as a weakly polar dielectric material with a low relative dielectric constant but high compressive strength, is particularly sensitive to these impurities. The complex composition within the air gaps leads to an uneven distribution of electric field strength, facilitating electron and ion collisions that can trigger ionization. Once ionization reaches a critical level, breakdown occurs, thereby compromising the cable's insulation performance.<sup>[4][5]</sup> As illustrated in Figure 2, bubble sizes typically range from a few microns to hundreds of microns. To obtain more pronounced experimental results, we varied bubble sizes as an experimental parameter to observe changes in electric field strength.<sup>[6]-[8]</sup>

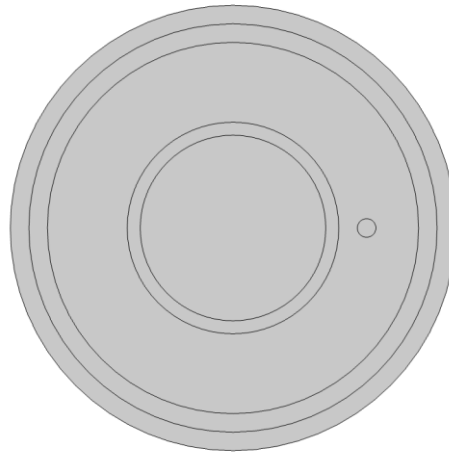


Figure 2: Simulation model of air gap defects

As shown in Figure 3, the bubble with the diameter of 1mm is selected, and the bubble model is established at a certain position from the conductor shield layer, and a two-dimensional intercept line is made with the innermost layer of the XLPE as the starting point, the outermost layer of the XLPE as the end point, and the two-dimensional intercept line passing vertically through the centre of the bubble circle, so as to observe the results of the simulation experiments of the different distributions of the bubbles.<sup>[9]-[11]</sup>

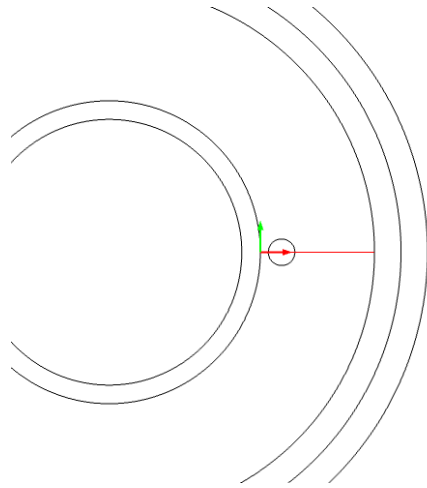


Figure 3: Two-dimensional cross-section of air gap defects

### 3. Simulation results and analysis

#### 3.1 Simulation results without air gap

Utilizing the finite element software COMSOL for simulation and analysis, we obtained the electric field intensity distribution graph for an XLPE cable without any defects, as illustrated in Figure 4. The results clearly indicate that the electric field within the XLPE cable is substantial, with the highest electric field intensity occurring at the interface between the wire core and the XLPE layer. Referring to the radial electric field distribution curve depicted in Figure 5 for a cable without defects, it is evident that the electric field intensity peaks near the conductor shield layer. As we move away from this layer, the electric field intensity exhibits a decreasing trend. Notably, the maximum recorded electric field intensity stands at approximately 3.2kV/mm.

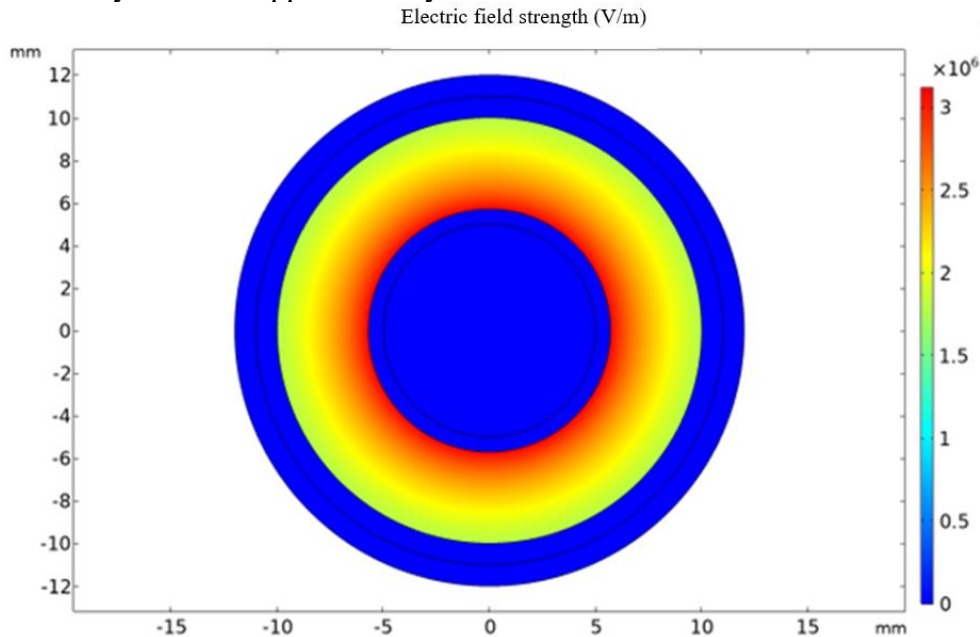


Figure 4: Distribution of defect-free electric field

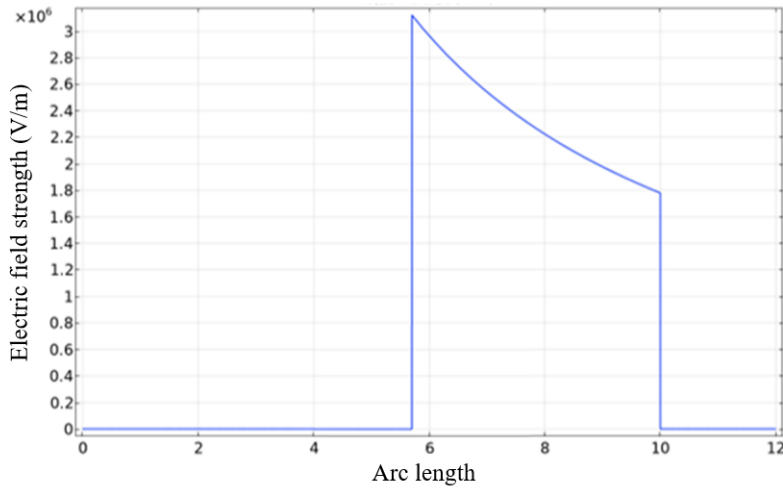


Figure 5: Radial electric field distribution curve in the absence of defects

### 3.2 Simulation results with air gap

#### 3.2.1 Effect of air gap size variation on field strength

Within the XLPE insulation layer, a circular insertion of 1mm diameter was introduced., and the distance from the semiconductor layer for the position of  $L = 1\text{mm}$  on the drawing of small holes to simulate the air gap defects, Figure 6 shows that the air gap at the field strength of the field appeared to be a significant distortion. Observed in the transverse direction, the potential in the vicinity of the air gap and insulation layer interface decreases sharply, but the electric field strength at the air gap is greater than that in the absence of the air gap. Observed in the radial direction, the maximum value of the field strength appears at the core of the conductor, and the electric field strength gradually decreases from the main insulation from the inside to the outside, and the near-ground side is 0. Figure 7 illustrates the radial electric field distribution of the air gap defect. Since the relative permittivity of the air gap is smaller than that of the XLPE insulation layer, the electric field strength at the junction of the two regions suddenly increases to 3.61 KV/mm, which is about 12.8% higher than the maximum field strength value under normal conditions.

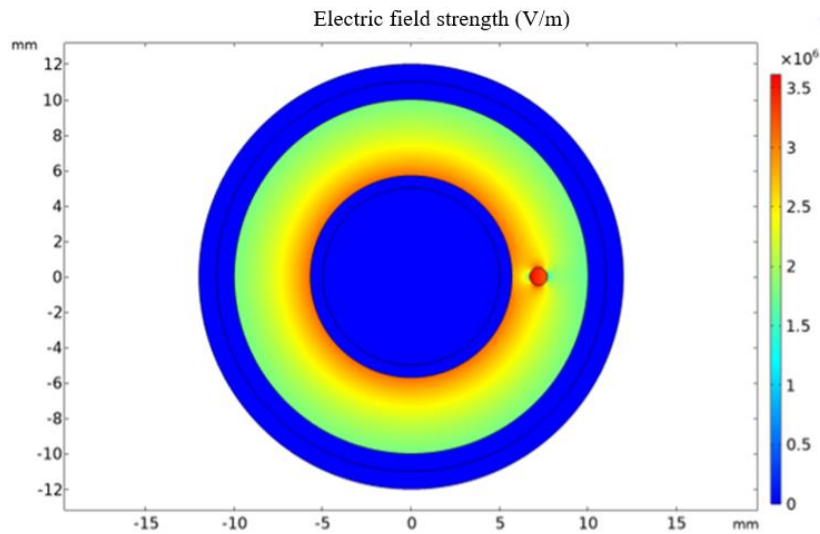


Figure 6: Electric field distribution of air gap defects ( $d=1\text{mm}$ ,  $L=1\text{mm}$ )

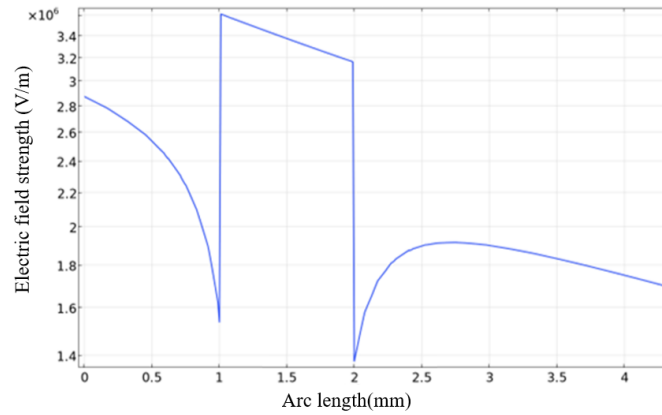


Figure 7: Radial electric field distribution curve of air gap defects (d=1mm, L=1mm)

### 3.2.2 Simulation results for different sizes of air gaps

In order to further analyse in depth the effect of bubble size variation on the electric field strength distribution in XLPE cables, as shown in Figure 8 and Figure 9, when the bubble diameter is reduced to 0.7 mm (at a distance of  $L = 1$  mm from the semiconducting layer), the degree of electric field strength aberration induced by such smaller bubbles is significantly reduced in comparison with larger defects in previous studies. This result suggests that a reduction in bubble size can reduce the potential threat to the safe operation of cables.

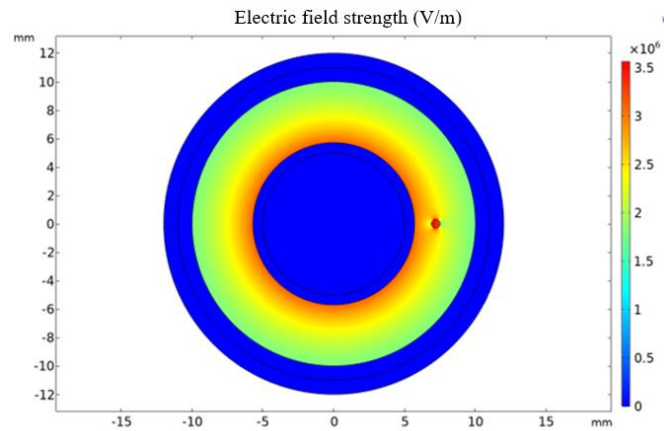


Figure 8: Air gap defects' electric field dispersal (d=0.7mm, L=1mm)

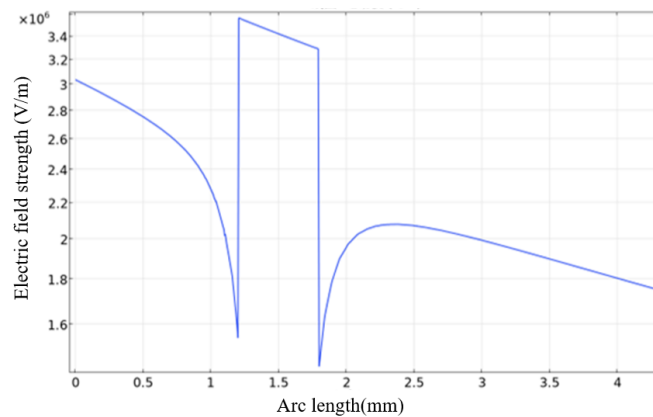


Figure 9: Air gap defect electric field distribution curve (d=0.7mm, L=1mm)

Next we increased the bubble size (1.4 mm diameter) as shown in Figure 10 and Figure 11. When the bubble diameter increases to 1.4 mm, its maximum field strength distortion value is the maximum distortion value. Compared to the smaller defects studied previously, the degree of electric field strength distortion induced by this larger bubble is reduced, which can be seen that there is a diameter between the air gap diameter of 0.6 mm and 1.4 mm, making the field strength distortion the most severe in the cable.

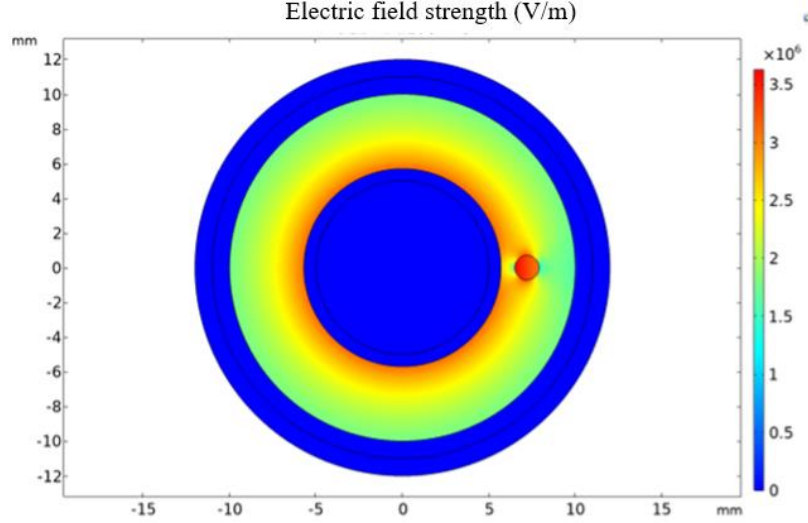


Figure 10: Electric field distribution of air gap defects (d=1.4mm, L=1mm)

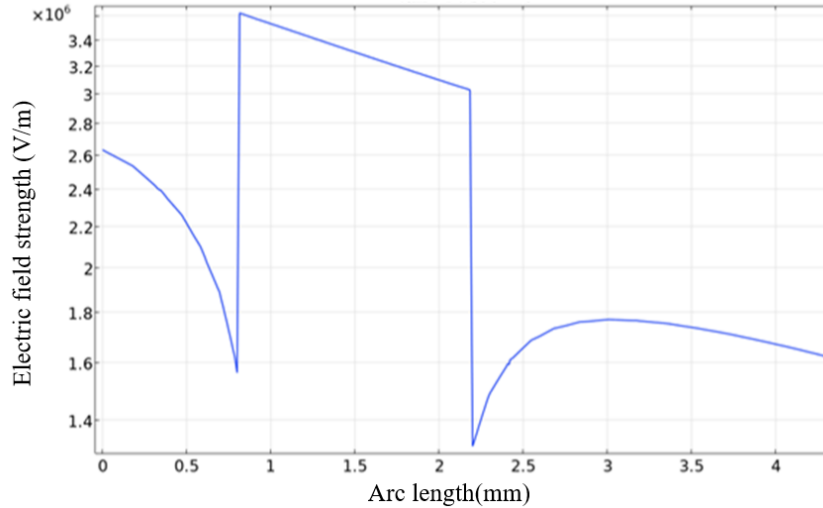


Figure 11: Air gap defects' electric field curve (d=1.4mm, L=1mm)

In order to more accurately describe the change in electric field intensity with the size of the air gap, the size is changed when the position of the air gap defects is unchanged, and a total of six air gap models are created. To make the results of the simulation more clear, the position of the air gap is set to 1mm from the semiconductor layer,  $L=1\text{mm}$ , and the diameter of the air gap is set to  $d_1=0.125\text{mm}$ ,  $d_2=0.25\text{mm}$ ,  $d_3=0.5\text{mm}$ ,  $d_4=1\text{mm}$ ,  $d_5=1.5\text{mm}$ ,  $d_6=2\text{mm}$ , to simulate the effect of different radial dimensions on the electric field distribution.

Figure 12 shows in detail the maximum field strength values and their distribution ranges for different bubble diameters. It can be clearly observed that when the air gap diameter is less than 1mm,



with the increase of the bubble diameter, the maximum field strength value shows an obvious upward trend, while the regional range of electric field distortion decreases; when the air gap diameter is more than 1mm, with the increase of the bubble diameter, the maximum field strength value shows an obvious downward trend, while the regional range of electric field distortion increases. This finding not only deepens the understanding of the electric field distribution characteristics of XLPE cable, but also provides a more refined theoretical basis for cable manufacturing, operation and maintenance.

According to Figure6, when the diameter is 0.125mm, the maximum field strength is 3.99KV/mm; when the diameter is 1mm, the maximum field strength increases to 4.1KV/mm; when the diameter is 2mm, the maximum field strength decreases to 3.86KV/mm. With the increase of the air gap diameter, the electric field strength first increases and then decreases.

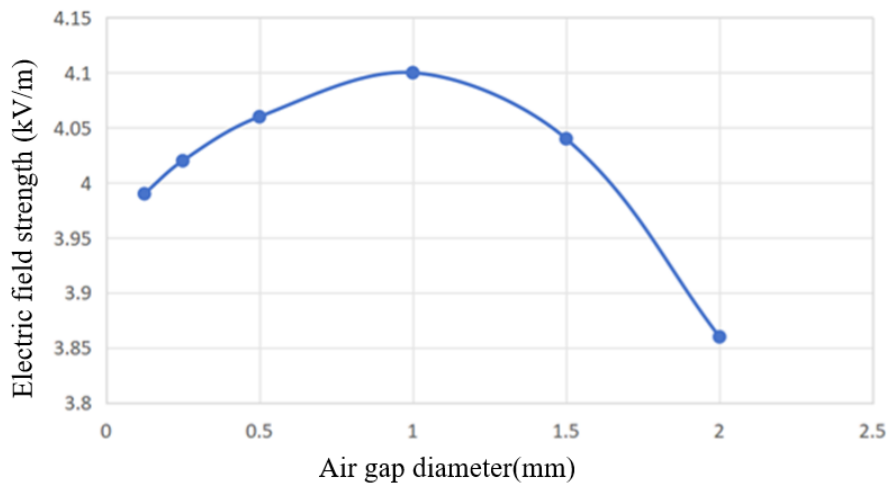


Figure 12: Electric field distribution curves of air gap defects with varying radii

In summary, bubble size is one of the key factors affecting the distribution of electric field strength in XLPE cables. By finely controlling the bubble size, the degree of electric field distortion can be effectively reduced and the safety and reliability of the cable can be improved. Therefore, the formation and size of air bubbles should be strictly controlled during cable manufacturing and installation to ensure normal operation and long-term stability of the cable.

### 3.2.3 Influence of the size of the distance between the air gap defects inside the cable insulation and the conductor shield on the electric field intensity

To further investigate the effect of changing the air gap position on the electric field strength distribution in XLPE cables, the size of the air gap is fixed and only the position of the air gap in the cable is changed, in order to analyse in depth the difference in electric field distortion caused by the change in position. Through simulation analysis, we can observe how the distribution of electric field strength and the degree of distortion change with the change in air gap position. This will help us to more accurately assess the potential impact of the air gap at different locations on the safe operation of the cable. Through this study, we aim to gain a more comprehensive understanding of the mechanisms by which the air gap position affects the characteristics of the electric field distribution within the cable.

Firstly, the size of the air gap is set at a diameter of 1 mm and the air gap is set at a radial distance from the semiconducting layer of  $L = 2$  mm for the model shown in Figures 13 and 14, which has a maximum distortion value of 3.16 KV/mm in field strength and a maximum distortion rate of 134%.

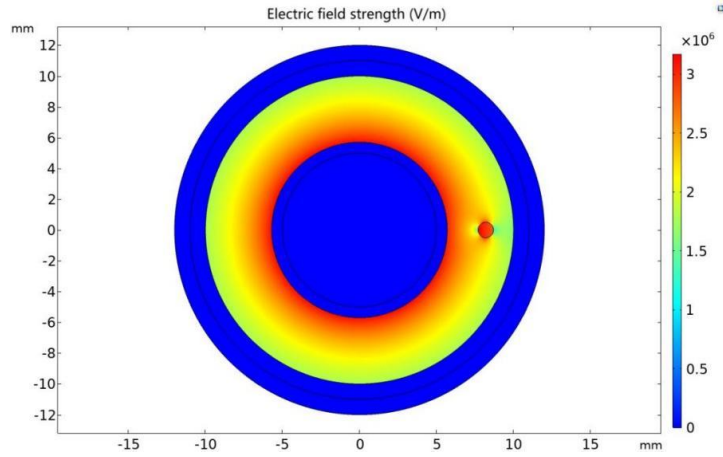


Figure 13: Electric field distribution of air gap defects (d=1mm, L=2mm)

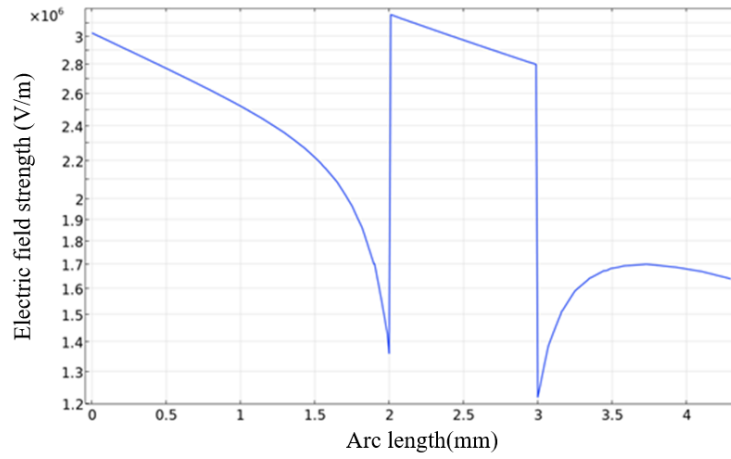


Figure 14: Air gap defect electric field distribution curve (d=1mm, L=2mm)

Secondly, keeping the diameter of the air gap model as 0.5mm in size and changing the air gap distance radial distance from the semi-conducting layer  $L=3\text{mm}$  model, there are simulation results that show that the maximum field strength value of its field strength is  $2.75\text{KV/mm}$  as shown in Figures 15 and 16. The maximum distortion of its field strength is 129%.

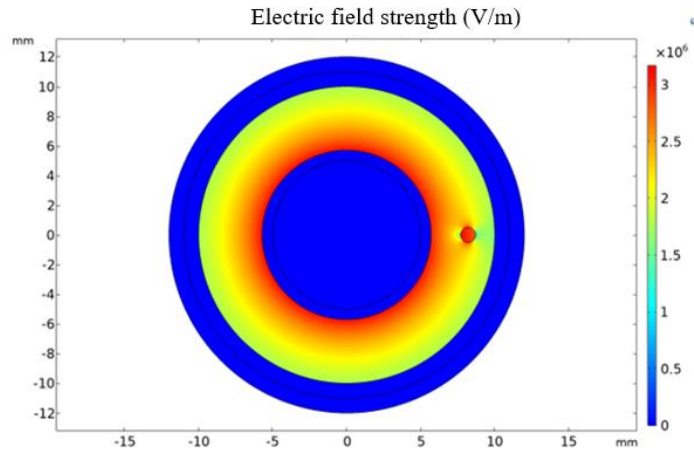


Figure 15: Electric field distribution of air gap defects (d=1mm, L=3mm)

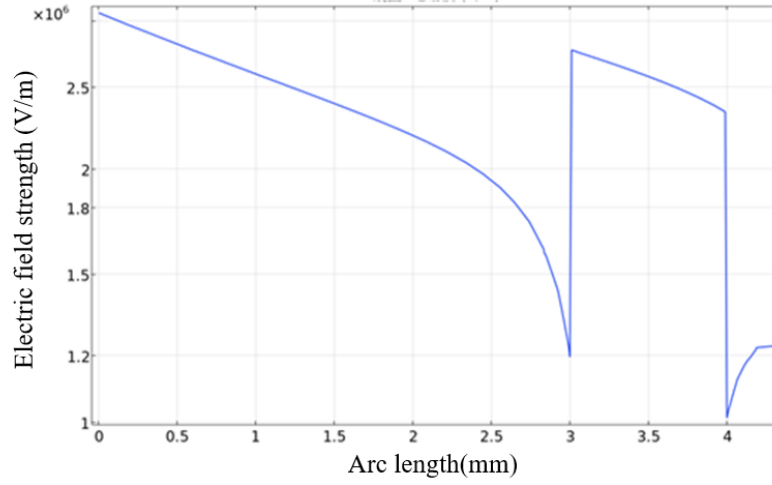


Figure 16: Air gap defect electric field distribution curve (d=1mm, L=3mm)

Finally, this study keeps the size of the air gap unchanged and changes its distance to the semiconducting layer, a total of six air gap models are established, the diameter of which are all 0.5 mm, and the distance to the semiconducting layer are L1=0.5 mm, L2=1 mm, L3=1.5 mm, L4=2 mm, L5=2.5 mm and L6=3 mm, respectively, and the spatial location of the air gap is simulated with different values of the distance. <sup>[12][13]</sup> Taking the largest surface area of the semiconducting layer as the starting point and the outermost layer of the XLPE as the end point, and drawing a two-dimensional intercept line perpendicular to the central of the circle through the bubble, it is possible to simulate the results shown in Figure 17, which shows that the electric field strength at the air gap insulation produces an aberration, and the value of the maximum field strength inside the same sized air gap decreases with increasing distance. At the same time, the rate of reduction of the maximum electric field strength at the air gap is accelerated as the air gap is further away from the semiconducting layer.

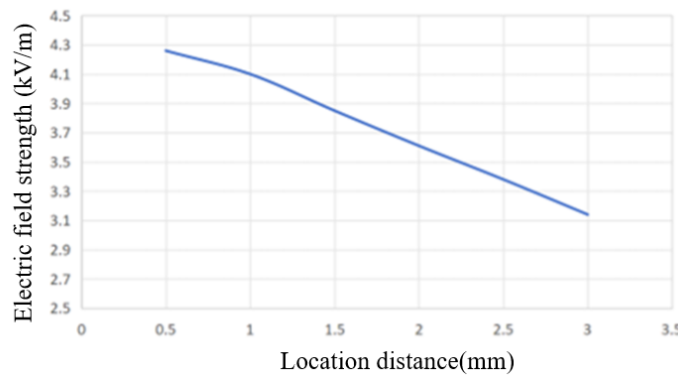


Figure 17: Electric field distribution curves for air gap defects at different locations

#### 4. Conclusions

In order to investigate the effect of bubble defects in the XLPE layer of cross-linked polyethylene (XLPE) high-voltage cables on the electric field strength, in this paper, using COMSOL finite element software, simulation experiments were carried out on bubble defects of different sizes and locations, and the corresponding electric field strength distributions were also observed and analysed, and the following conclusions can be drawn:

(1) When there are no defects, the electric field strength inside the XLPE cable is smaller with increasing distance from the semiconducting layer.

(2) When there is an air gap defect, the electric potential near the intersection surface of the bubble and the XLPE layer decreases sharply, but the electric field intensity is greater than that without the bubble; with the location of the air gap closer to the outer surface of the XLPE layer of the cable, the air gap at the aberration is the weaker, and the electric field intensity is also reduced.

(3) When there is an air gap defect, the field strength distribution of the air gap defect is related to the radius size and spatial location. The same size air gap location distance and the maximum field strength are inversely proportional; with the same distance, as the air gap diameter increases, the electric field strength first increases and then decreases.

The future feasibility and future development direction of this study are as follows:

(1) Refined manufacturing control: The results of the study show that by finely controlling the size and position of air bubbles during the manufacturing process, the electric field distortion can be effectively reduced, and the reliability and safety of the cable can be improved. This provides a theoretical basis for improving the cable manufacturing process.

(2) Improvement of detection technology: The bubble defect analysis method proposed in the study can be used to improve the existing cable detection technology, develop more sensitive detection equipment, and timely detect and treat bubble defects.

(3) Research on multiple types of defects: In the future, the research can be extended to other types of defects (e.g. cracks, impurities, etc.) to establish a more comprehensive defect model, which will further improve the safety of XLPE cables.<sup>[14]</sup>

(4) Simulation of actual working conditions: The research results will be applied to actual working conditions, combined with the simulation and analysis of complex factors in the actual application environment, to improve the practical application of the research results.

(5) Development of an intelligent monitoring system: Based on the research results, an intelligent monitoring system will be developed to realise real-time monitoring and early warning of the cable status, detect potential problems in advance and prevent failures.

## References

- [1] Hung C L , Hsiao Y K , Tu C C .Investigation of 4H-SiC UMOSFET Architectures for High Voltage and High Speed Power Switching Applications[J].Materials Science Forum, 2023.
- [2] Hu Xinyu, Zhu Hui, Chen Xingang. Simulation study of electric field of defects in 10 KV XLPE cable joints[J]. Journal of Chongqing University of Technology(Natural Science), 2022, 36(02):171-178.
- [3] Bondarenko G G , Kristya V I , Savichkin D O ,et al.Simulating the Effect of Field Electron Emission from a Cathode with a Thin Dielectric Film on Its Sputtering in a Gas Discharge in an Argon and Mercury Vapor Mixture[J].Journal of Surface Investigation: X-ray, Synchrotron and Neutron Techniques, 2024, 18(2):327-332.DOI:10.1134/ S1027451024020058.
- [4] YE Yongsheng, Deng Tengfei, LI Forgingneng, LIAO Jinren. Overview of high-voltage cable materials and their preparation process for electric vehicles [J]. Automotive components, 2021, (01):114-117.
- [5] Lu Guojun, Xiong Jun, Ruan Banyu, Liu Gang, Chen Zhijuan. Experiment on detecting 10kV cross-linked polyethylene cable joints containing defects by oscillating wave voltage method [J]. Guangdong Electric Power, 2011, 24(06): 18-22.
- [6] Shen Chen. Research and development of partial discharge data analysis system for XLPE cable based on map feature recognition [D]. Shanghai Jiao Tong University, 2018.
- [7] Hu K, Lu ZF, Yang FY, Zhang L, Zhang YX. Simulation of typical defects and partial discharge research of high-voltage DC XLPE cable[C]. Proceedings of Zhejiang Electric Power Society 2018 Annual Excellent Papers, 2018:324-331.
- [8] Zhao Peng. Design of high-voltage DC cross-linked polyethylene (XLPE) cable accessories based on COMSOL simulation [D]. China Electric Power Research Institute, 2018.
- [9] Xia JF, Shi NN, Sun JS. Simulation analysis of the effect of typical defect patterns on electric field distortion in the main insulation of high-voltage XLPE cables [J]. Wire and Cable, 2022, (06):1-6.
- [10] Zhang Long, Zhang Wei, Li Ruipeng, Li Hongjie. Simulation and electric field analysis of termination defects in

10kV XLPE cables [J]. *Insulation Materials*, 2014, 47(04):83-88.

[11] Liu LY. *Research on defect modeling and intelligent identification method of urban underground transmission cable joints* [D]. Shijiazhuang Railway University, 2023

[12] Hua Liangwei, Feng Yong, Mao Yan, Wang Ying, Cao Xiaolong. *Discussion on the performance of cross-linked polyethylene insulating materials and extrusion process*[J]. *Wire and Cable*. 1999, (06):42-45

[13] Du Hao, Guan Honglu, Chen Xiangrong, Hou Shuai, Yang Min, Wang Xin. *Partial discharge characteristics of typical defects in cross-linked polyethylene cables under DC voltage*[J]. *High Voltage Technology*, 2021, 47(02):555-563.

[14] Mikrut P , Zydron P .*Numerical Modeling of PD Pulses Formation in a Gaseous Void Located in XLPE Insulation of a Loaded HVDC Cable*[J].*energies*, 2023, 16(17).